Modern Solar Facilities – Advanced Solar Science, 359–362
F. Kneer, K. G. Puschmann, A. D. Wittmann (eds.)

Nanoflare model of emission line radiance distributions in active region coronae

H. Safari[1,2,*], D. E. Innes[2], S. K. Solanki[2], and A. Pauluhn[3]

[1]Institute for Advanced Studies in Basic Sciences, Zanjan, Iran
[2]Max-Planck-Institut für Sonnensystemforschung, Katlenburg-Lindau, Germany
[3]Paul Scherrer Institut, Villigen, Switzerland
[*]*Email:* hsafary@iasbs.ac.ir

Abstract. Nanoflares are small impulsive bursts of energy that blend with and possibly make up much of the solar background emission. Determining their overall contribution is central to understanding the heating of the solar corona. Here, a simple nanoflare model based on three key parameters: the flare rate, the flare damping time, and the power-law slope of the flare energy frequency distribution has been used to simulate emission line radiances observed by SUMER in the corona above an active region. The three lines analysed, Fe XIX, Ca XIII, and Si III have very different formation temperatures, damping times and flare rates but all suggest a power-law slope greater than 2. Thus it is possible that nanoflares provide a significant fraction of the flare energy input to active region coronae.

1 Introduction

Nanoflares were postulated first by Levine (1974) and later by Parker (1988) to be the source of the solar corona's background heat. The majority would be small fluctuations on the overall background and impossible to detect, so their energy has been estimated by extrapolating the energy frequency distribution of larger flares. The energy frequency distribution of larger flares tends to follow a power-law distribution

$$\frac{dN}{dE} \sim E^{-\alpha}, \tag{1}$$

where dN is the flare number in energy interval dE. The energy of small flares dominates if $\alpha > 2$ (Hudson 1991). The standard method to evaluate α is to evaluate the energy of many flares in a series of observations and then plot their frequency in bins of energy dE. The majority of analyses based on this type of event counting deduce $\alpha \approx 1.7$, a value smaller than the critical 2 (Lin et al. 1984; Shimizu 1995; Aschwanden & Parnell 2002). These results may, however, be misleading. For example, Parnell (2004) demonstrated that one can obtain α ranging from 1.5 to 2.6 for the same dataset using different but still reasonable sets of assumptions for the analyses.

Here we take an alternative approach and model UV radiances observed by SUMER in an active region corona, assuming that the radiance fluctuations and the nearly constant 'background' emission are caused by small-scale stochastic flaring (Pauluhn & Solanki 2004, 2007). The model has successfully been applied to UV radiance fluctuations in the quiet

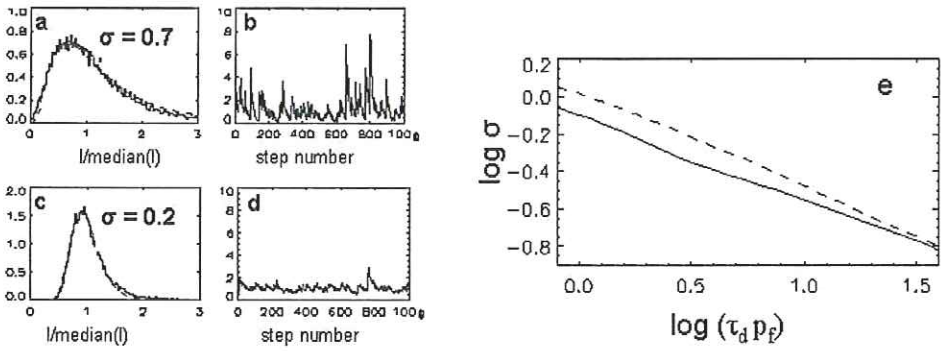

Figure 1. Simulation radiance distributions (**a, c**) for the light curves (**b, d**) on their right and (**e**) the dependence of shape parameter σ on $\tau_d p_f$ for $\alpha = 1.6$ (dashed) and $\alpha = 2.4$ (solid).

Sun (Pauluhn & Solanki 2007). The lines chosen, Fe XIX (7 MK), Ca XIII (1 MK) and Si III (0.05 MK), cover two decades in formation temperature. In a previous paper, event counting in the Fe XIX dataset deduced an $\alpha \approx 1.8$ (Wang et al. 2006).

2 The Model

A detailed outline of the model and assumptions are given in Pauluhn & Solanki (2007). Basically, flares with a power-law frequency distribution in radiance are assumed to erupt with a frequency, p_f, and then decay with a damping time, τ_d. The radiance observed is the sum of all overlapping radiances.

For a large number of independent random flares, the radiance distribution is lognormal:

$$\rho(x) = \exp\left(-\frac{(\log(x))^2}{2\sigma^2}\right) \Big/ \left(\sigma x \sqrt{2\pi}\right), \tag{2}$$

where σ is the shape parameter. Small σ (< 0.3) indicates a symmetric distribution due to high background emission caused by either a long damping time, τ_d, or a high flare frequency, p_f. Examples are given in Fig. 1a-d. σ is inversely proportional to $\sqrt{\tau_d p_f}$ (Pauluhn & Solanki 2007) with a slight α dependence as shown in Fig. 1e. The radiance distribution can be used to obtain the value $\tau_d p_f$ to within $\approx 20\%$.

2.1 Wavelet analysis

Since our model is random no periods are expected and this is observed when analysing the model light curves. We notice however that the steepness of the wavelet global power spectrum at high frequencies depends inversely on the damping time, so can be used to determine τ_d to within $\approx 20\%$. Global power spectra for different τ_d are shown in Fig. 3e with the global power spectra of the data overplotted.

Figure 2. EIT 195 Å image taken on 17 Sep 2000 of observed active region showing the position of the SUMER slit (black vertical line).

3 Observations

The active region corona was observed at a fixed position above the limb (Fig. 2) in the three lines, Fe XIX, Ca XIII and Si III by SUMER. Observations were made over periods of 14 hours with an exposure time of 1.5 min. Therefore a typical period would consist of about 500 exposures. Observations were made over several days but for this analysis we look at data from the 14 hours when the active region was closest to the limb for the Fe XIX and Ca XIII. The Si III data were taken on the following day when a number of small surge-like events were seen above the limb. More details of the observational setup are given in Wang et al. (2006). The images in Fig. 3a, show the time series of radiance seen along the slit for the analysed periods.

For each line, radiance distribution functions were computed from the complete dataset and fitted with the lognormal function. Using the different σ's we are able to obtain $\tau_d p_f$ from the relationship plotted in Fig. 1e. Then using the wavelet analysis to get the τ_d, we obtain the p_fs. Given the τ_d and p_f, we run the flare simulations for various α's. This gives light curves that can be compared with our SUMER observations. In Figs. 3b,c,d we show simulated and observed light curves. As α increases, the background becomes smoother and single flares become more prominent. A foolproof technique to quantify this effect is the next stage of our analysis. For the moment, we can say that the simulations with $\alpha = 2.4$ look the most realistic. Those with $\alpha = 1.6$ have too much background variation, whereas those with $\alpha = 3$ do not have enough larger flares.

Acknowledgements. H. S. acknowledges warm hospitality and financial support during his research visit to the solar group, MPS, Katlenburg-Lindau.

References

Aschwanden, M. J. & Parnell, C. E. 2002, ApJ, 572, 1048
Hudson, H. S. 1991, Solar Phys., 133, 357
Levine, R. H. 1974, ApJ, 190, 457
Lin, R. P., Schwartz, R. A., Kane, S. R., Pelling, R. M., & Hurley, K. C. 1984, ApJ, 283, 421
Parker, E. N. 1988, ApJ, 330, 474
Parnell, C. E. 2004, in ESA SP-575: SOHO 15 Coronal Heating, 227
Pauluhn, A. & Solanki, S. K. 2004, in ESA SP-575: SOHO 15 Coronal Heating, ed. R. W. Walsh, J. Ireland, D. Danesy, & B. Fleck, 501

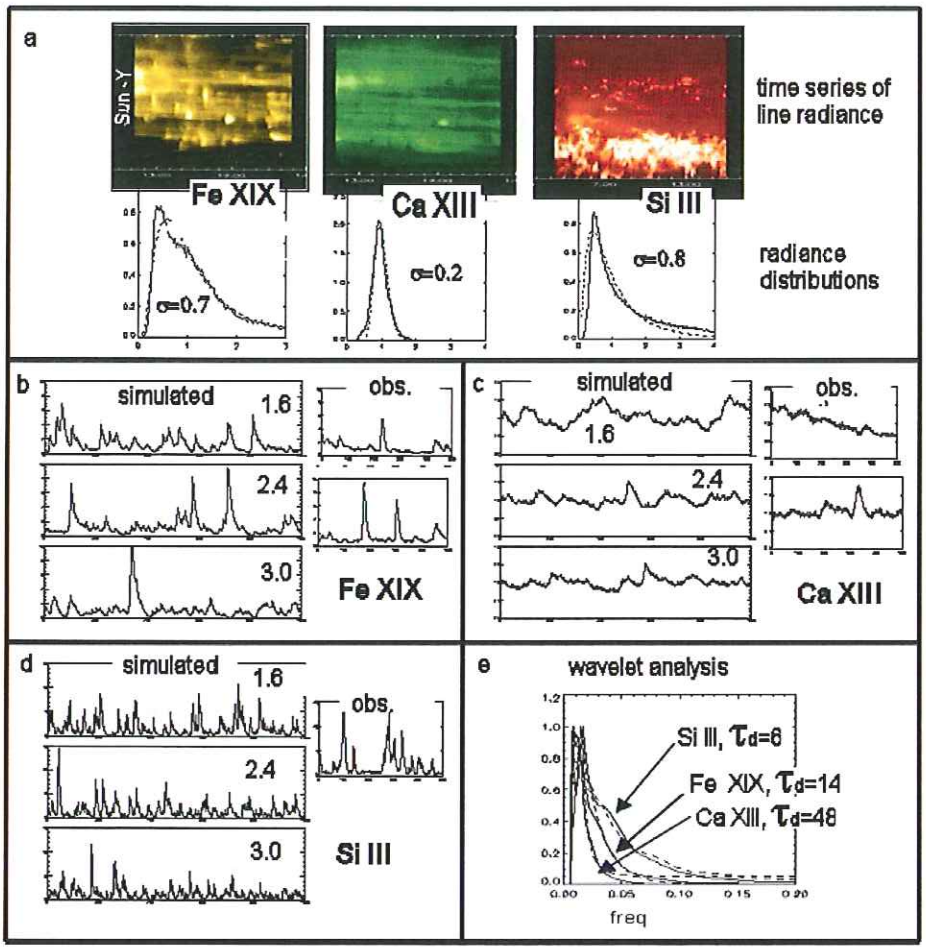

Figure 3. SUMER observations and modelling. (**a**) From left to right: Fe XIX, Ca XIII, Si III time series of line radiance along the spectrometer slit together with the corresponding radiance distributions of the data in the pictures above (solid) and the lognormal fit (dashed). (**b**) Fe XIX simulations with $\tau_d = 14$, $p_f = 0.1$ and $\alpha = 1.6, 2.4, 3.0$ and observed light curves taken from two of the rows in **a**. (**c**) Ca XIII simulations with $\tau_d = 48$, $p_f = 0.6$ and $\alpha = 1.6, 2.4, 3.0$ and observed light curves. (**d**) Si III simulations with $\tau_d = 6$, $p_f = 0.2$ and $\alpha = 1.6, 2.4, 3.0$ and a typical observed light curve. (**e**) Wavelet global power spectra for light curves with different τ_d (solid) and for our data (dashed). The simulation light curves are the average over about fifty 500 step light curves. The data are the average of all rows along the slit of the 500 step block on 17-Sep (Fe XIX, Ca XIII) and on 18-Sep (Si III).

Pauluhn, A. & Solanki, S. K. 2007, A&A, 463, 311
Shimizu, T. 1995, PASJ, 47, 251
Wang, T. J., Innes, D. E., & Solanki, S. K. 2006, A&A, 455, 1105